







## Upper Jurassic – Lower Cretaceous of eastern Wollaston Forland, North-East Greenland: a distal marine record of an evolving rift

Jussi Hovikoski<sup>1,2</sup> , Jon R. Ineson<sup>1</sup> , Mette Olivarius<sup>3</sup> , Jørgen A. Bojesen-Koefoed<sup>4</sup> , Stefan Piasecki<sup>1,5,6</sup> , Peter Alsen<sup>3</sup> 

<sup>1</sup>Department for Geophysics and Sedimentary Basins, Geological Survey of Denmark and Greenland (GEUS), Copenhagen, Denmark; <sup>2</sup>Geological Survey of Finland (GTK), Espoo, Finland; <sup>3</sup>Department for Geo-energy and Storage, Geological Survey of Denmark and Greenland (GEUS), Copenhagen, Denmark; <sup>4</sup>Department for Mapping and Mineral Resources, Geological Survey of Denmark and Greenland (GEUS), Copenhagen, Denmark; <sup>5</sup>Globe Institute, University of Copenhagen, Copenhagen, Denmark; <sup>6</sup>Retired

### Abstract

Two drill cores spanning the Upper Jurassic – Lower Cretaceous succession in Wollaston Forland, North-East Greenland, offer an insight into mud accumulation in an evolving distal fault block. Previous studies have revealed the presence of long-lasting black mudstone accumulation extending through the oxygen-restricted early rift and rift climax phases (Bernbjerg and Lindemans Bugt Formations). Here, we present a detailed description of the sedimentary succession extending into the late syn-rift settings (Palnatokes Bjerg and Stratumbjerg Formations). The results indicate that the Kimmeridgian – lower Volgian early rift-phase was characterised by suspension settling and millimetre-scale event deposition in a tectonically affected, prodeltaic offshore setting. The event-related depositional processes are recorded by starved wave ripples, scour-and-fill structures, putative mud-floccule ripples and mud-dominated gravity-flow deposits. During the middle Volgian – Ryazanian rift climax, the depositional environment evolved into a narrow half-graben that was detached from the proximal depocentre flanking the deltaic coastline, itself dominated by coarse sediment. The correlative sedimentary facies in the detached half-graben are bioclastic and pyrite-rich black mudstones, which document suspension settling and gravity-flow or mass-wasting deposition in sub-storm wave-base slope and basin-floor environments. Black mudstone sedimentation ended abruptly in the late Ryazanian when the accumulation of condensed, bioturbated deep marine marls coincided with broader oceanographic reorganisation concomitant with waning rift activity in the west. Deposition of red bioclastic mudstones with a common gravity-flow component characterised the Hauterivian, potentially representing final draping of the submerged fault block crest. The top of the cored succession is demarcated by dark grey bioturbated mudstones of Barremian age, reflecting the onset of regionally continuous deep marine mud accumulation in thermally subsiding basins. Although superficially monotonous, the mudstone-dominated succession reveals a highly dynamic depositional system that reflects changing sediment transport processes during almost a full rift cycle.

### 1. Introduction

Although mudstones form most of the Earth's sedimentary record, they remain less understood than most other rock types (Schieber *et al.* 2007). This is unfortunate because mudstones form important archives of Earth's climatic and oceanographic processes and crises and are economically valuable, hosting petroleum source rocks and hydrocarbons and forming seals in hydrocarbon, groundwater and carbon storage reservoirs (Potter *et al.* 2005). Traditionally, mud has been regarded as being deposited via suspension settling under low-energy conditions (Potter *et al.* 1980). However, particularly since the early 2000s, flume-tank experiments and detailed observations from the modern sea floor, and from ancient successions, have revealed that mud accumulation can take place during much

**\*Correspondence:** [jussi.hovikoski@gtk.fi](mailto:jussi.hovikoski@gtk.fi)

**Received:** 03 Mar 2023

**Revised:** 12 Sep 2023

**Accepted:** 26 Sep 2023

**Published:** 21 Dec 2023

**Keywords:** Late Jurassic, Early Cretaceous, Bernbjerg Formation, Lindemans Bugt Formation, Palnatokes Bjerg Formation, Stratumbjerg Formation, mudstone, Greenland

#### Abbreviations

API: American Petroleum Institute units

BI: bioturbation index

GR: gamma ray

WEGF: wave-enhanced gravity-flow

GEUS Bulletin (eISSN: 2597-2154) is an open access, peer-reviewed journal published by the Geological Survey of Denmark and Greenland (GEUS). This article is distributed under a [CC-BY 4.0](https://creativecommons.org/licenses/by/4.0/) licence, permitting free redistribution, and reproduction for any purpose, even commercial, provided proper citation of the original work. Author(s) retain copyright.

**Edited by:** Karen Dybkjær (GEUS, Denmark)

**Reviewed by:** Guy Plint (Western University, Canada) and Paul Smith (Oxford University Museum of Natural History, UK)

**Funding:** See page 18

**Competing interests:** See page 18

**Additional files:** None

more varied hydrodynamic conditions than previously thought (Kineke *et al.* 1996; Wright *et al.* 2001; Bentley & Nittrouer 2003; Macquaker & Bohacs 2007; Schieber *et al.* 2007; Ichaso & Dalrymple 2009; Schieber & Southard 2009; Schieber & Yawar 2009; Macquaker *et al.* 2010; Ghadeer & Macquaker 2011; Plint *et al.* 2012; Plint 2014; Yawar & Schieber 2017). Most notably, such studies have shown that mud can be transported as, and deposited from, bedload transport, which can generate subtle sedimentary structures (e.g. cross-lamination, normally graded lamina sets, structureless ungraded mud laminae and convergent lamination) that remain overlooked in the sedimentary record. This can be particularly true in outcrop studies where mudstone successions are typically poorly exposed relative to coarser facies and tend to appear homogenous due to weathering.

The Upper Jurassic – Lower Cretaceous depositional record of eastern Wollaston Forland, North-East Greenland (Fig. 1), provides an exceptional window into mudstone deposition under changing paleoenvironmental conditions. The area experienced a protracted rift phase that started in the Middle Jurassic, reached a climax during the Late Jurassic and waned progressively during Jurassic–Cretaceous boundary times and through the Early Cretaceous (Surlyk 1978, 1990, 2003). As a result of rift evolution, the basin geometry changed from a regionally continuous suboxic shelf setting to a series of narrow half-grabens that were subsequently affected by thermal subsidence and transgression. Whilst the fill of the proximal half-grabens was coarse-grained, being characterised by major conglomeratic submarine fan-delta systems (Surlyk 1978, 2003; Henstra *et al.* 2016), the distal fault blocks were mud-filled, stagnated and

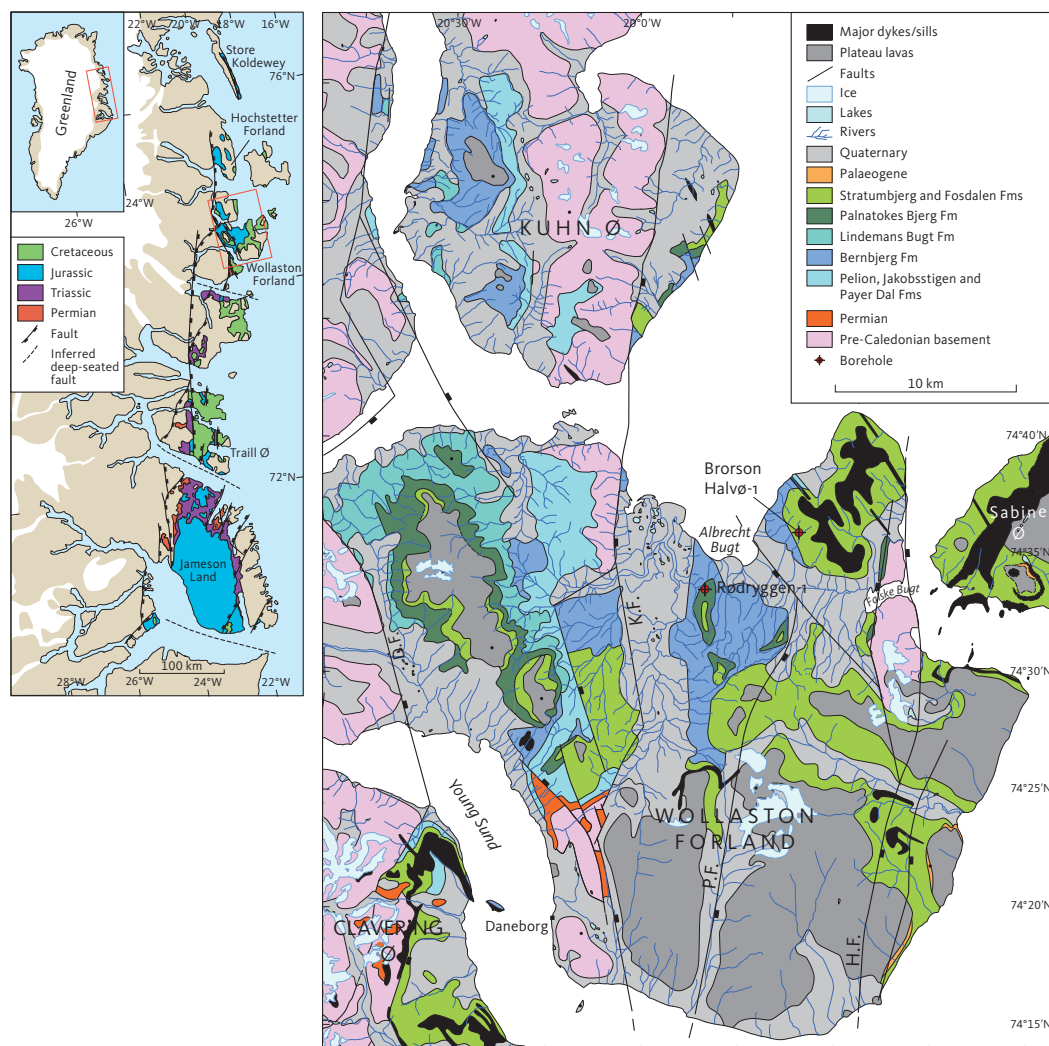


**Fig. 1** Location maps. **Left:** Geological overview map of East and North-East Greenland showing the location of the study area (red box) and the dominant Late Jurassic – Early Cretaceous faults. **Right:** Simplified geological map of Wollaston Forland showing the positions of the Rødryggen-1 and Brorson Halvø-1 boreholes. **K.F.:** Kuhn fault. **P.F.:** Permpas Fault. **H.F.:** Hühnerbjerg Fault. **D.F.:** Dombjerg Fault. The position of the coastline was primarily dictated by the Dombjerg Fault during the Late Jurassic, whilst the Kuppel and Hühnerbjerg Faults were the most important structures controlling the distal half-graben architecture. Reproduced from Bojesen-Koefoed *et al.* (2023a, this volume, fig. 1).



detached from the coastal gravity-flow systems (Pauly *et al.* 2013; Hovikoski *et al.* 2023; Bojesen-Koefoed *et al.* 2023, this volume; Olivarius *et al.* 2023, this volume). The subsequent rift waning and thermal subsidence were associated with improved ventilation and deposition of deep marine mudstones.

All these tectonostratigraphic phases are recorded in the fully cored boreholes Rødryggen-1 and Brorson Halvø-1, which were drilled in two contrasting locations within a distal half-graben (Figs 1, 2). Full core recovery has yielded pristine preservation of the Kimmeridgian to lower Barremian mudstone-dominated succession, allowing detailed documentation of the sedimentary facies of the dominant, organic-rich black mudstone succession (Bernbjerg and Lindemans Bugt Formations), as well as the gradation to upper Ryazanian bioturbated mudstones (Palnatokes Bjerg and Stratumbjerg Formations). The sedimentary facies of the black mudstone interval were recently summarised in Hovikoski *et al.* (2023) in which the wider implications

of this subsurface record are developed with respect to the development of anoxia in the region during rift-ing. The aim of this complementary paper is to present a comprehensive description of the depositional facies and processes in this unexposed and previously unknown distal marine setting.

## 2. Stratigraphy and depositional setting

The cored section covered by the Rødryggen-1 and Brorson Halvø-1 boreholes spans the Kimmeridgian to lower Barremian interval, which is divided into four formations: (1) the Bernbjerg Formation, (2) the Lindemans Bugt Formation (the new Storsletten Member; Alsen *et al.* 2023, this volume), (3) the Palnatokes Bjerg Formation (the Albrechts Bugt Member and the Rødryggen Member) and (4) the Stratumbjerg Formation (Fig. 2).

The age of the Bernbjerg Formation is late Oxfordian to early Volgian, and it comprises a thick black

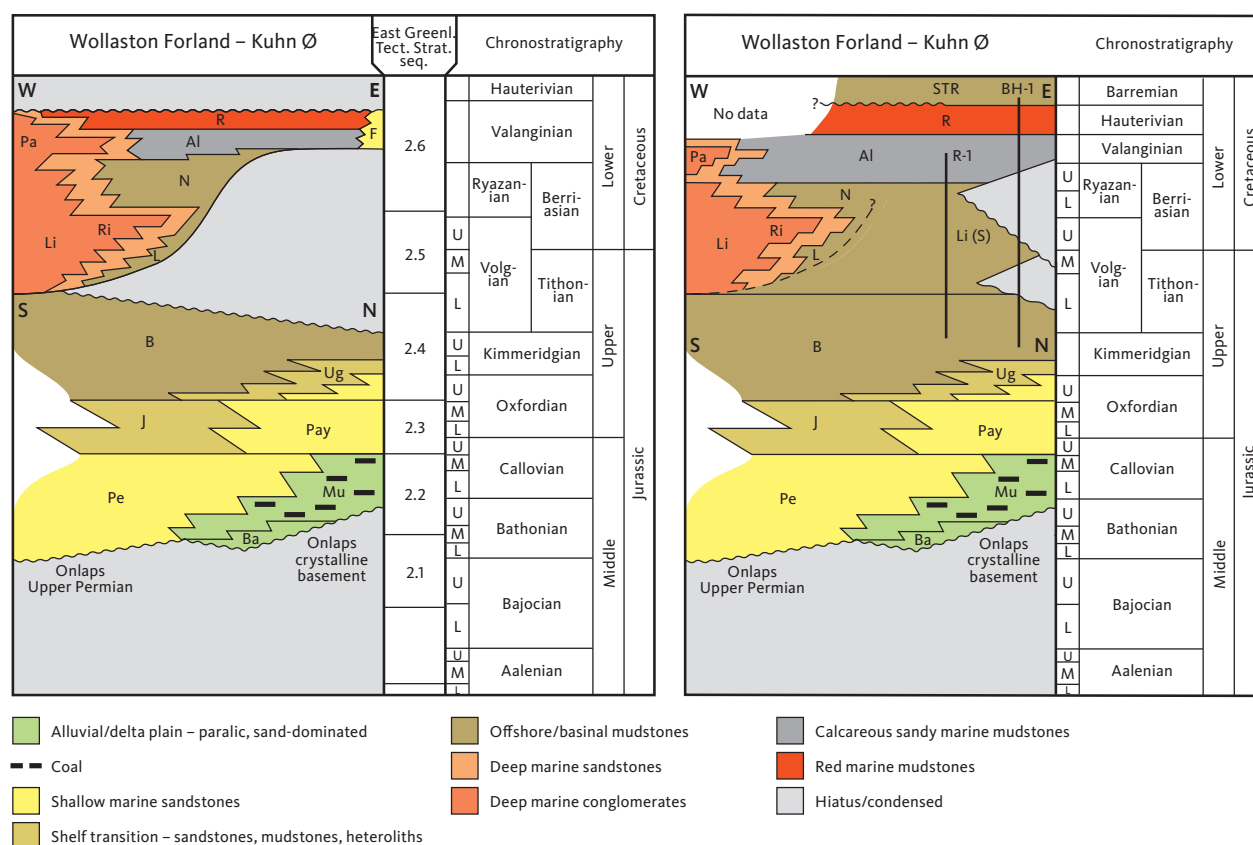


**Fig. 2** Stratigraphic models of the Wollaston Forland – Kuhn Ø area. **Left:** the conceptual stratigraphic scheme of Surlyk (2003) based on outcrop study. **Right:** the revised scheme after drilling of the Rødryggen-1 and Brorson Halvø-1 boreholes and incorporating changes introduced by Surlyk *et al.* (2021). The revised succession is much more complete and richer in marine mudstone (brown colour) than previously envisaged. **East Greenl. Tect. Strat. Seq.:** East Greenland Tectono-stratigraphic sequence. **U:** Upper/upper. **M:** Middle/middle. **L:** Lower/lower. Lithostratigraphic abbreviations are as follows: **Al:** Albrechts Bugt Member. **B:** Bernbjerg Formation. **Ba:** Bastians Dal Formation. **F:** Falskebugt Member. **J:** Jakobsstigen Formation. **L:** Laegeites Ravine Member. **Li:** Lindemans Bugt Formation. **Li (S):** Lindemans Bugt Formation (Storsletten Member). **Mu:** Muslingebjerg Formation. **N:** Niesen Member. **Pa:** Palnatokes Bjerg Formation (Young Sund Member). **Pay:** Payer Dal Formation. **Pe:** Pelion Formation. **R:** Rødryggen Member. **Ri:** Rigi Member. **Str:** Stratumbjerg Formation. **Ug:** Ugpik Ravine Member. **Black vertical lines** indicate the schematic location and stratigraphic extent of the Rødryggen (**R-1**) and Brorson Halvø-1 (**BH-1**) boreholes. Reproduced from Bojesen-Koefoed *et al.* 2023b (this volume).

mudstone shale succession (500–600 m) that accumulated in a tectonically influenced shelf setting (Sykes & Surlyk 1976; Surlyk *et al.* 2021). Previous sedimentological studies of outcrop sections have reported the presence of a dysoxic to anoxic or euxinic shelf setting with occasional storm influence during Oxfordian–Volgian times (Surlyk & Clemmensen 1975, 1983). Similarly, the previous core-based study pointed to a generally sub-oxic prodeltaic shelf environment (Hovikoski *et al.* 2023). Rifting intensified during the Volgian, which dissected the basin into a series of narrow, 10–30 km wide, westward tilted, fjord-like half-grabens (Vischer 1943; Surlyk 1978). Major conglomeratic submarine fan-delta systems (Lindemans Bugt Formation, Rigi Member; Surlyk 1978; Henstra *et al.* 2016) developed in the most proximal fault blocks reaching a maximum thickness of 2 km. The coeval paleoenvironmental development in more distal, eastern fault blocks remained poorly understood due to the lack of outcrops, but is well-recorded in the cores described here, which indicate deep basinal sedimentation and isolation from the coarse-grained proximal systems (Hovikoski *et al.* 2023). The mudstone-dominated succession that accumulated in this setting is referred to the new Storsletten Member of the Lindemans Bugt Formation (Alsen *et al.* 2023, this volume).

The rift climax started to wane in the west during the late Ryazanian, leading to the deposition of the Palnatokes Bjerg Formation (Surlyk 1978, 1984, 1990, 2003). The formation changes coincided with transgression and improved ventilation in the water column and oceanographic change with improved communication between the Boreal and Tethyan realms (Pauly *et al.* 2013). Sand-dominated gravity-flow deposits (Palnatokes Bjerg Formation, Young Sund Member) continued to accumulate in the proximal fault block, whereas fossiliferous mudstones (Albrechts Bugt and Rødryggen Members) accumulated in basinal areas and on submarine block crests (Surlyk 1978; Hovikoski *et al.* 2018). The Rødryggen-1 and Brorson Halvø-1 cores penetrate both the latter, fine-grained members, and new biostratigraphic data indicate a late Ryazanian to Hauterivian age for these deposits (Alsen *et al.* 2023, this volume). In the Brorson Halvø-1 core, the Palnatokes Bjerg Formation is gradationally overlain by a thin interval of uppermost Hauterivian – Barremian, sub-storm and wave-base bioturbated mudstones of the Stratumbjerg Formation (Bjerager *et al.* 2020). This formation crops out from Traill Ø in the south to Store Koldewey in the north and reaches its maximum thickness of 270 m in the Brorson Halvø area; the Stratumbjerg Formation was previously referred to as the ‘Mid-Cretaceous sandy shale sequence’ (Nøhr-Hansen 1993).

### 3. Methods

The Rødryggen-1 and Brorson Halvø-1 cores were sedimentologically and ichnologically described at a scale of 1:100. The sedimentological description included descriptions of lithology, grain size (visual estimation) and trends in grain size, primary and secondary sedimentary structures, bedding contacts and the identification of important stratigraphic surfaces. Diagenesis and authigenic minerals are described in Olivarius *et al.* (2023, this volume) and are integrated in facies descriptions. Ichnological data comprise description of ichnogenera, trace-fossil assemblage, cross-cutting relationships and bioturbation index (BI of Taylor & Goldring 1993). The BI provides a description of the degree to which original sedimentary fabric has been destroyed due to biogenic processes. This classification scheme allocates a numerical value ranging from 0 to 6 – the values correspond to the percentage of bioturbation (cf. Taylor & Goldring 1993). Undisturbed or non-bioturbated sedimentary fabrics are classified as BI 0 (0% reworked), while pervasively bioturbated media (100% reworked) are classified as BI 6. Intermediate levels of bioturbation are characterised using BI 1–5 and are defined as follows: BI 1, 1–4% reworked; BI 2, 5–30% reworked; BI 3, 31–60% reworked; BI 4, 61–90% reworked; BI 5, 91–99% reworked (Taylor & Goldring 1993). Locally, a lack of lithological contrast hindered accurate estimation of the degree of bioturbation. The age of the sediments is based on the biostratigraphy of Alsen *et al.* (2023, this volume).

### 4. Depositional facies

The two cored sections spanning the Bernbjerg, Lindemans Bugt, Palnatokes Bjerg and Stratumbjerg Formations are divided into seven facies (F1–7). The facies are grouped and described here according to the lithostratigraphic unit(s) in which they occur (Figs 3, 4), as follows:

- F1, F2, F3 and F7 Bernbjerg and Lindemans Bugt Formations
- F4 and F5: Palnatokes Bjerg Formation
- F6: Stratumbjerg Formation

#### 4.1 Bernbjerg and Lindemans Bugt Formations

The studied deposits of the Bernbjerg and Lindemans Bugt Formations are divided into four facies (F1, F2, F3 and F7) and five subfacies (F1A, F1B, F1C, F2A and F2B) based on their sedimentological and ichnological properties.

##### 4.1.1 Facies F1: mudstone

Three subfacies (F1A–C) are recognised in the mudstone facies (Fig. 5A–G).

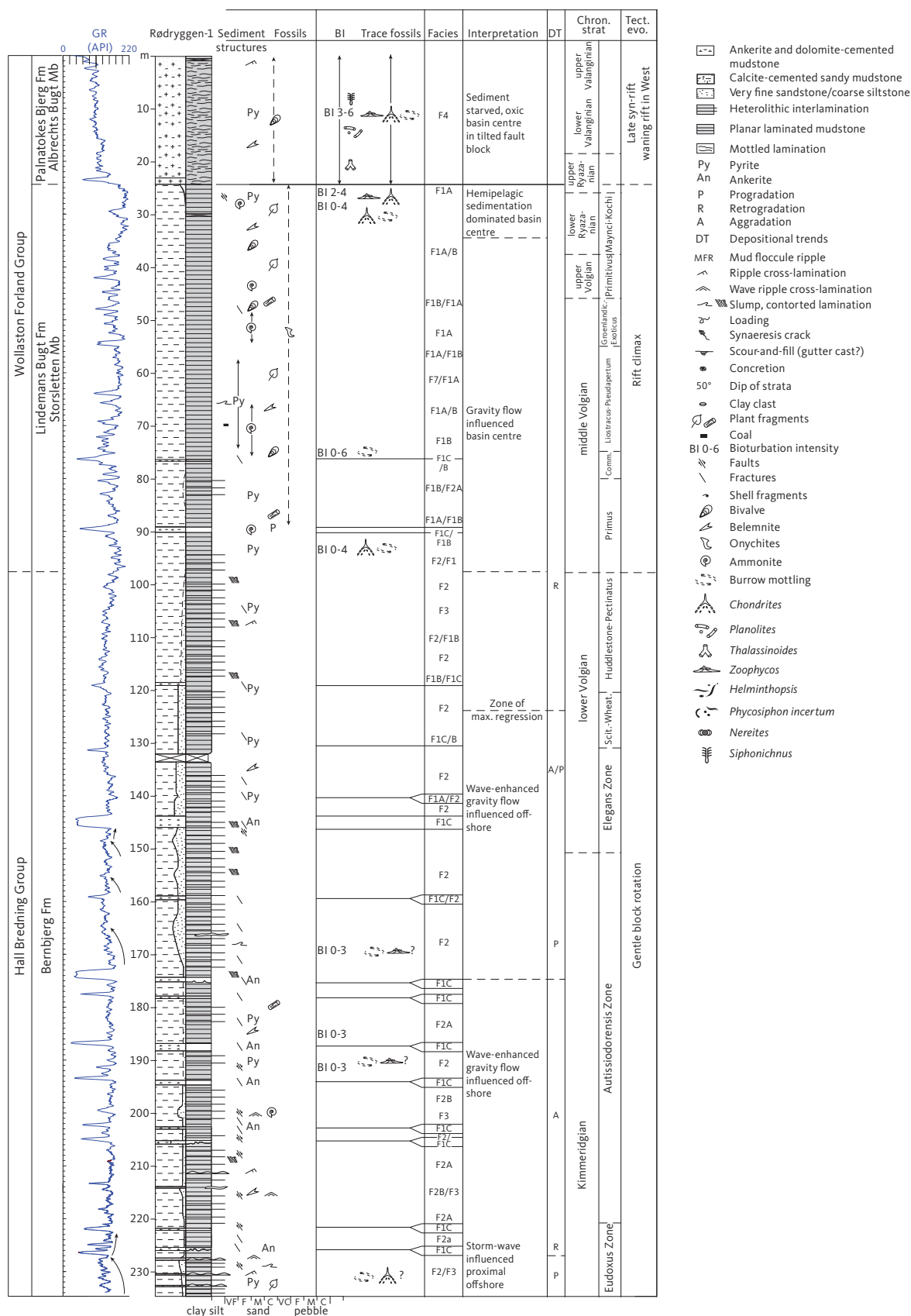


**Fig. 3** Sedimentological log of the Rødryggen-1 core. Note that the ammonite zones are here indicated with chronozone terminology, whereas in the text, ammonite zones are used. Modified from Hovikoski *et al.* (2023). **Chron. Strat.:** chronostratigraphy. **Tect. evo.:** tectonic evolution. **GR:** gamma ray. **Comm.:** Comminus Zone. **Scit.-Wheat.:** Scitulus-Wheatleyensis Zones. **Groenlandic.:** Groenlandicus Zone.

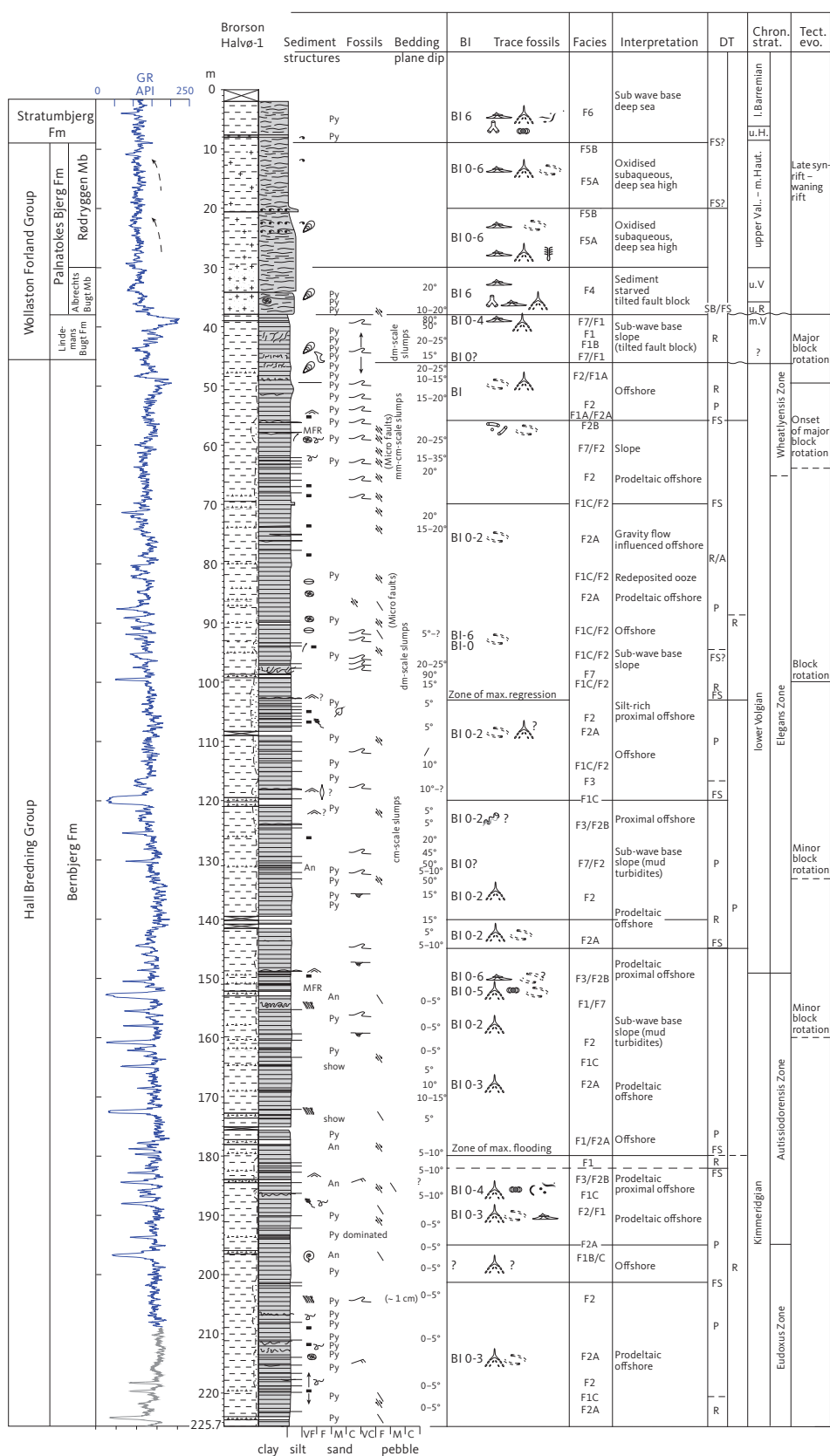


**Fig. 4** Sedimentological log of the Brorson Halvø-1 core. Modified from Hovikoski *et al.* (2023). Chronostratigraphic abbreviations: **l.**: lower, **m.**: middle, **u.**: upper, **Vol.**: Volgian, **R.**: Ryazanian, **V./Val.**: Valanginian, **H./Haut.**: Hauterivian. Legend in Fig. 3.



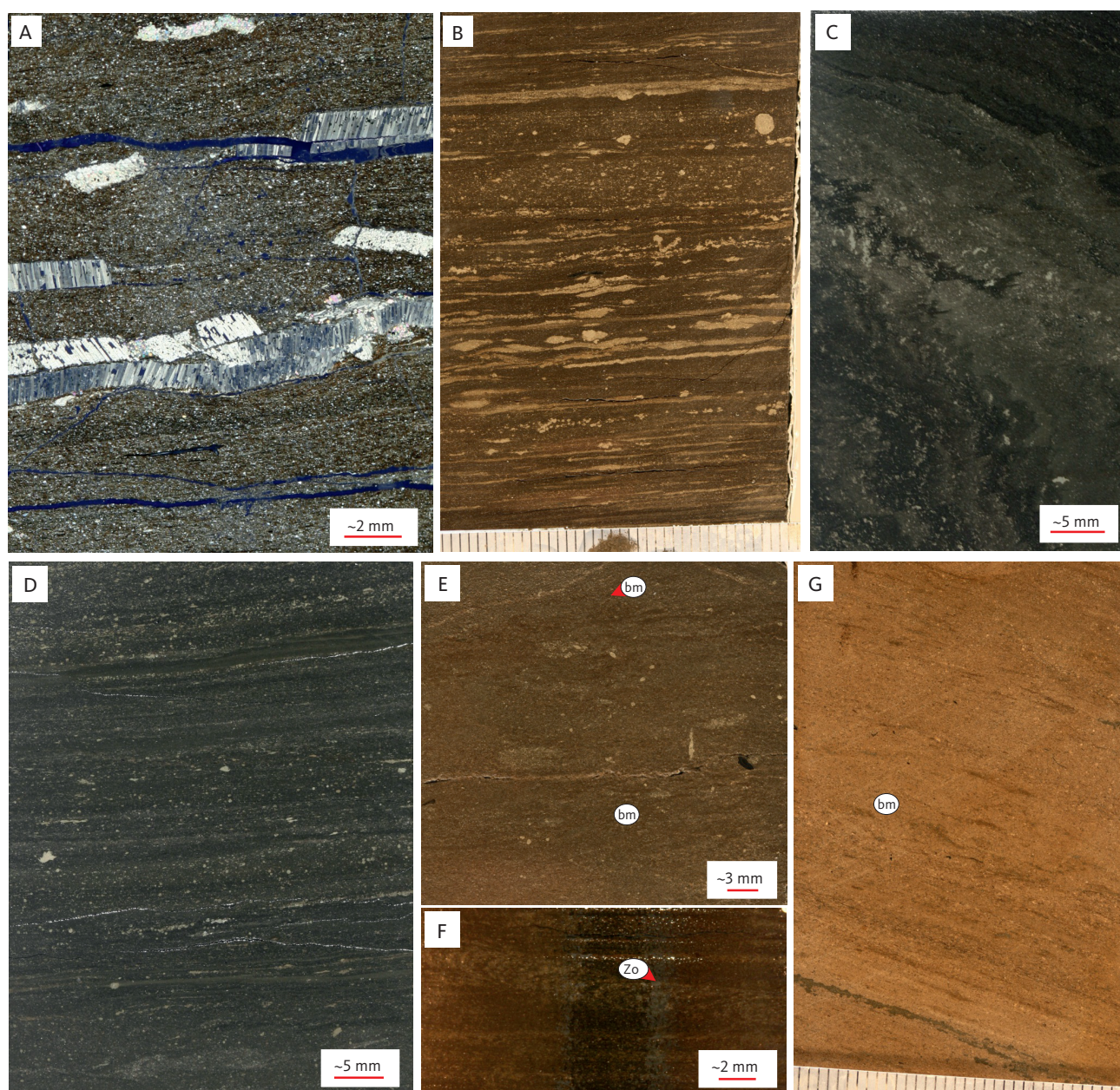


**Fig. 5** Facies F1. **A:** Laminated black mudstone with common inoceramid fragments. F1A, Rødryggen-1, 26.6 m. **B–D:** Examples of ‘colour-banded’ pyrite-rich mudstone of F1B. Fig. 5C illustrates slump-folded ankerite- and pyrite-rich mudstone. **B:** Rødryggen-1, c. 64 m. **C:** Brorson Halvø-1, c. 47.5 m. **D:** Brorson Halvø-1, 46 m. **E, F:** Bioturbated examples of F1AB. **E:** Rødryggen-1, ~ 29 m. **F:** Rødryggen-1, ~ 25.5 m. Panel F represents a gradational interval from Lindemans Bugt to Palnatokes Bjerg Formation. **G:** Laminated to bioturbated ankerite- and dolomite-cemented mudstone. Subfacies F1C, Rødryggen-1, 76.6 m. **bm:** burrow mottling. **Zo:** *Zoophycos*.

#### 4.1.1.1 Subfacies F1A: massive to laminated clayey mudstone

**Description:** F1A is a rare subfacies type occurring mainly in the Lindemans Bugt Formation (in the core intervals: Rødryggen-1 c. 97–24.4 m, Brorson Halvø-1 41–38 m; Figs 3, 4), where it typically forms centimetre- to metre-scale successions. It commonly occurs in association with F7 (slumps) and F1B (colour-banded mudstone), and less commonly with F2 (clay-silt heteroliths) in the Bernbjerg Formation (Fig. 4, 178 m).

F1A has the finest grain size of the described facies and typically shows the highest gamma-ray (GR) values of

the succession (>180 API; American Petroleum Institute units). It consists of dark grey to black, apparently structureless or faintly laminated clayey mudstone (Fig. 5A). Pyrite is locally common. Generally, the deposits appear to be unbioturbated or contain rare diminutive *Chondrites*, *Zoophycos* and indistinct mottling (BI 0–3; Fig. 5E, F). The transitional occurrences (F1A/F2A) in the Bernbjerg Formation are more commonly intensively micro-bioturbated with millimetre to sub-millimetre scale indistinct traces that are typically visible as laminae disruptions (BI 0–5). The estimation of BI and recognition of trace fossils was locally hampered by lack of lithological contrast and



poorly preserved core (rubble). Finally, F1A is fossil-rich, bearing ammonites, belemnites and bivalves.

*Interpretation:* The lithology and sedimentary structures (e.g. laminated mud), concentration of marine fossils and ichnological properties are compatible with a marine, sub-storm wave-base, oxygen-deficient basinal environment characterised by hemipelagic suspension settling (see Hovikoski *et al.* 2023 for redox data). The close association with F7 (slumps) in the middle Volgian of the Brorson Halvø-1 section suggests a drowned slope setting in a tilted fault block at this location.

The bioturbated, intermediate occurrences in the Bernbjerg Formation are interpreted as dysoxic offshore sediments based on ichnological and sedimentological characteristics as well as the stratigraphic occurrence of the facies.

#### 4.1.1.2 Subfacies F1B: colour-banded mudstone

*Description:* Subfacies 1B is common in the Lindemans Bugt Formation in Rødryggen-1 (core depth 90–30 m). In the Brorson Halvø-1 core, F1B is rare, forming a thin interval in the middle Volgian (core depth 43 m). In addition, a single occurrence of F1B transitional to F1C was recorded at around 152 m in the Bernbjerg Formation. In both of the latter instances, the subfacies is also associated with slumps (F7).

F1B alternates gradationally with F1C and F1A, being an intermediate facies type between these two subfacies. On the GR log, F1B shows intermediate values commonly ranging between 100 and 150 API. This facies consists of interlaminated clayey mudstone, pyrite and ankerite-rich mudstone (see Olivarius *et al.* 2023, this volume), which leads to the characteristic colour banding of this facies (Fig. 5B, D). Moreover, lensoidal laminae and possible low-relief cross-lamination occur locally, but their conclusive documentation is hampered by soft-sedimentary deformation and concretionary structures (e.g. pyrite nodules) that obscure primary micro-facies. Bioclasts, consisting mainly of marine elements (e.g. onychites (belemnoid hooks), ammonites and bivalves), are also common. Pyrite is abundant. F1B typically appears to be unbioturbated (BI 0) and shows small-scale soft-sedimentary deformation structures (micro-slumps consisting of contorted lamination and micro-scale loading structures). The determination of bioturbation intensity is hampered locally, however, by lack of lithological contrast in black mudstone-dominated intervals.

*Interpretation:* Abundant small-scale soft sedimentary deformation, structureless mud laminae up to a few mm thick and local lenticular laminae suggest that deposition was probably partly derived from muddy gravity flows rather than being solely the result of hemipelagic

suspension fallout. Similarly, the alternation between stratified and structureless micro-facies suggests alternating transport processes, potentially driven by changing turbulence under decelerating mud flows (Plint 2014). The gravity flows were probably facilitated by the increasing depositional gradient due to late early Volgian – early Ryazanian fault block development (Surlyk 1978, 2003).

The localised ankeritic laminae probably reflect alteration of rare primary laminae rich in bioclasts (e.g. calcispheres; see Section 4.1.1.3; Olivarius *et al.* 2023, this volume). Considering the sedimentological and ichnological properties described here, coupled with the stratigraphic occurrence of the facies, F1B is interpreted to represent the accumulation of oxygen-deficient, basinal to slope mudstone in a tilted fault-block setting (see Section 5. Discussion).

#### 4.1.1.3 Subfacies F1C: ankerite- and dolomite-rich mudstone

*Description:* F1C is a common facies type in both core sections in the Kimmeridgian and lower Volgian (Rødryggen-1 230–70 m, Brorson Halvø-1 220–48 m; Fig. 5G). It occurs most commonly as decimetre-scaled intervals. On the GR logs, F1C is readily identified by anomalously low GR peaks (<50 API) that sometimes occur within an interval of overall high GR readings (at the base of an upward-coarsening interval) or at the very top of coarsening-upward successions. In addition, F1C occurs in trendless successions.

F1C consists of ankerite- and dolomite-cemented mudstone, which characteristically shows interlaminated mudstone and bioclast-rich mudstone; the bioclasts are replaced by pyrite and ankerite (see Olivarius *et al.* 2023, this volume). Poorly preserved, their typical circular cross-section is suggestive of calcispheres, although some vase-shaped cross-sections resemble calpionellids. Locally, F1C shows soft sediment deformation. Pyrite and apatite are locally common (e.g. 89.8 m in Rødryggen-1; Olivarius *et al.* 2023, this volume).

Bioturbation intensity ranges from unbioturbated to intensive burrow-mottling (BI 0–6; e.g. Brorson Halvø-1, 150 m; Fig. 5G). Burrow mottling contains indistinct c. 1 mm wide, horizontal to sub-horizontal trace fossils, which produce a mottled fabric. These are tentatively assigned to *Zoophycos*, because of (1) locally visible chevron-shaped structures, which may point to the presence of spreite, and (2) despite their diminutive size, they can in places be followed laterally through the width of the core, suggesting the presence of a lobe rather than an individual burrow. Estimation of bioturbation intensity in F1C is locally hampered by concretionary structures related to ankerite and dolomite formation.

*Interpretation:* The enrichment of bioclastic material, authigenic minerals (phosphate) and locally high

bioturbation intensity is best explained by reduced sedimentation rates (condensation). This interpretation is supported by the occasional stratigraphic occurrence of F1C at the very top or base of parasequences, which could point to a reduced sedimentation rate during either transgressive events, tectonic reorganisation or both. However, local soft sediment deformation features and the close association with slumps (F7) suggest that some of the F1C layers (e.g. Brorson Halvø-1, 100–80 m) may represent redeposited calcareous ooze that was originally deposited as a pelagic drape on the eastern sediment-starved, incipient block crest, following the onset of block rotation.

#### 4.1.2 Facies F2: interstratified claystone, siltstone and sandstone

**Description:** F2 is the dominant facies type in the Kimmeridgian – lower Volgian Bernbjerg Formation in the Rødryggen-1 cored section (234.5 to c. 97 m; Fig. 3), where it typically forms several metres thick aggradational (i.e. trendless) successions, and is also well-represented in this formation in the Brorson Halvø-1 core (225.7–45 m; Fig. 4). It is a transitional facies type with F3 (see Section 4.1.3) and can be gradationally or erosionally interbedded with F3. In addition, F2 is locally intercalated with F1C. On the GR log, F2 typically represents aggradational successions displaying relatively uniform GR values (c. 140–160 API). Locally, intervals dominated by F2 show stacked funnel-shaped GR patterns, a few metres thick (e.g. Rødryggen-1, 175–148 m; Fig. 3). F2 is most commonly unbioturbated, but locally, sporadic diminutive burrow mottling is recorded (BI 0–2).

F2 is subdivided into two subfacies: F2A, consisting of laminated mudstone (Fig. 6A, B), and F2B, which comprises interlaminated, very fine-grained sandstone or coarse siltstone and claystone and is characterised by lenticularity and basal erosional contacts (Figs 6C–H, 7A, B).

##### 4.1.2.1 Subfacies F2A: parallel-laminated clay and silt

**Description:** F2A is a common facies type in the Bernbjerg Formation. It forms millimetre- to centimetre-thick intervals occurring intergradationally between F1 and F2B. Together, these subfacies form aggradational (trendless) successions, or subtle, up to a few tens of metres thick, upward-coarsening successions (e.g. Rødryggen-1, 175–148 m; Brorson Halvø-1, 140–120 m).

F2A consists of fine-grained heterolithic interlamination, typically parallel-laminated siltstone and claystone (Fig. 6A). Lamina pinch-outs and erosional scours are rare or absent. Thin (c. 1 mm), tabular, normally graded siltstone–claystone couplets are present locally. Moreover, the transitional expressions (F2A–F2B gradation) show increasing silt content and lamina thickness, and the appearance of normally graded lamina sets a few

millimetres thick, which may laterally grade into scour-based, normally graded siltstone–claystone lamina sets (F2B). The deposits often appear unbioturbated or bear indistinct burrow mottling; rare diminutive *Zoophycos*, *Chondrites* and ?*Phycosiphon* occur in places (BI 0–5; Fig. 6A, B). Disseminated pyrite and particularly coalified wood fragments are common locally. F2A differs from F2B in that it lacks (1) signs of erosion, (2) sandstone, (3) clear normal grading and (4) laminae convergence, pinch-outs or lenticularity.

**Interpretation:** In F2A parallel lamination dominates, with no indications of erosion. As in F1A, the deposits are bioturbated locally with possible diminutive *Zoophycos*, *Chondrites* and indistinct sub-millimetre scale burrow mottling, which is in line with a dysoxic, generally low energy environment (e.g. Martin 2004; Boyer & Droser 2011; Schieber & Wilson 2021; see also Hovikoski *et al.* 2023 for redox data). The normally graded, tabular siltstone–claystone couplets that lack erosional scour are interpreted as the most distal expression of thin mud-dominated gravity flows (see Section 4.1.2.2 Subfacies F2B). The transitional variants showing graded lamina couplets that may grade laterally into erosionally based siltstone–claystone lamina sets suggest that this type of interlamination is partly related to weak traction deposition. The interpreted depositional mechanism is the gravity-flow component of wave-enhanced gravity-flow (WEGF) currents as described by Macquaker *et al.* (2010; see Section 4.1.2.2 for discussion). These wave-initiated flows possibly extended some distance below storm wave base as slope-maintained gravity-flow currents.

In summary, considering the sedimentological and ichnological characteristics as well as the stratigraphic position, subfacies F2A is interpreted to record a low-energy dysoxic offshore environment that periodically experienced dilute, muddy gravity-flow events.

##### 4.1.2.2 Subfacies F2B: cross-laminated – lenticularly laminated silt and clay

**Description:** F2B is a common subfacies type in the Brorson Halvø-1 core. It forms millimetre- to decimetre-scale successions and is commonly interbedded with F2A or F3. It usually occurs as a dominant subfacies in the top part of coarsening-upward successions (see Section 5. Discussion). F2B forms erosionally based upward-fining lamina sets a few millimetre thick, which may grade laterally into F2A over the width of the core. It is a broad subfacies dominated by interlaminated claystone–siltstone and lenses of siltstone, characterised by lamina truncations, low-relief erosional scours, lamina pinch-outs and down-lapping to top-lapping lamina contacts (Fig. 6C–H).



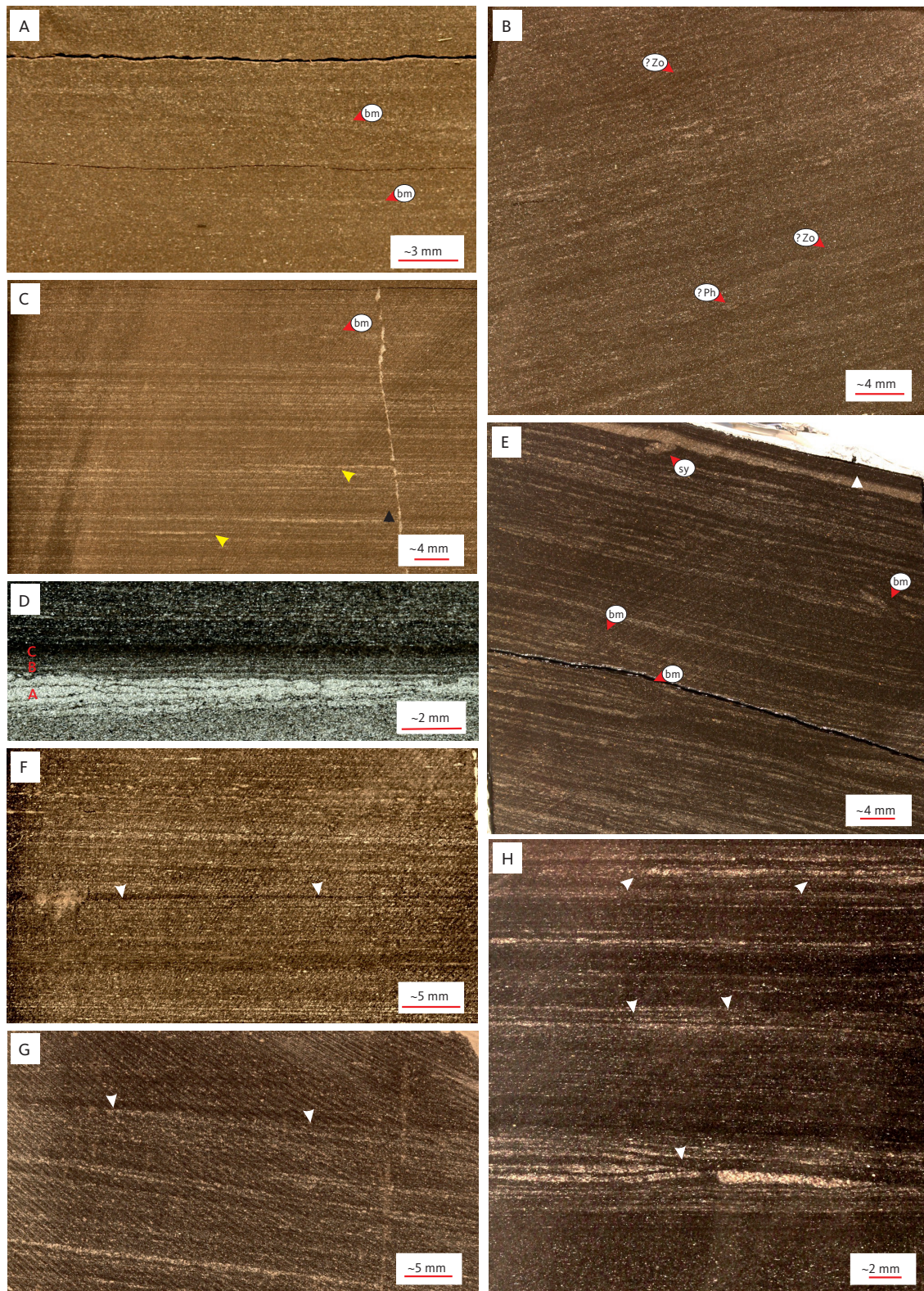


**Fig. 6** Facies F2. **A:** Laminated mudstone with local burrow mottling (**bm**). F2A, Rødryggen-1, c. 190 m. **B:** Laminated to bioturbated mudstone (F2). Biogenic structures are interpreted to include diminutive *Zoophycos* (**?Zo**) and *Phycosiphon* (**?Ph**). Brorson Halvø-1, c. 186 m. **C:** Laminated silt and clay of F2B, showing normally graded laminae sets (**black triangle**), lenticular laminae and erosional contacts (**yellow arrow**). Top of photo shows an interval of F2A with burrow mottling. Rødryggen-1, c. 231.5 m. **D:** Thin section image illustrating a typical tripartite division of a normally graded laminae set: a basal, erosionally based, cross-laminated very fine-grained sand or coarse silt lamina (unit A), parallel laminated silt and clay (unit B) and a clay-rich mud layer (unit C). F2B, Rødryggen-1, 206.8 m. **E:** Burrow mottling, visible as laminae disruption, in heterolithic interlamination. **Sy:** synaeresis crack. **White triangle:** normally graded laminae set. Brorson Halvø-1, 106 m. **F–H:** Facies examples illustrating laminae terminations (**white arrows**) and convergent lamination in F2B, suggesting the presence of ripple cross-lamination in mudstone. The lowermost cross-lamination in H contains sand and thus represents a transient example to F3. **F:** Rødryggen-1, 232 m. **G:** Brorson Halvø-1, c. 150.5 m. **H:** Brorson Halvø-1, 215 m.



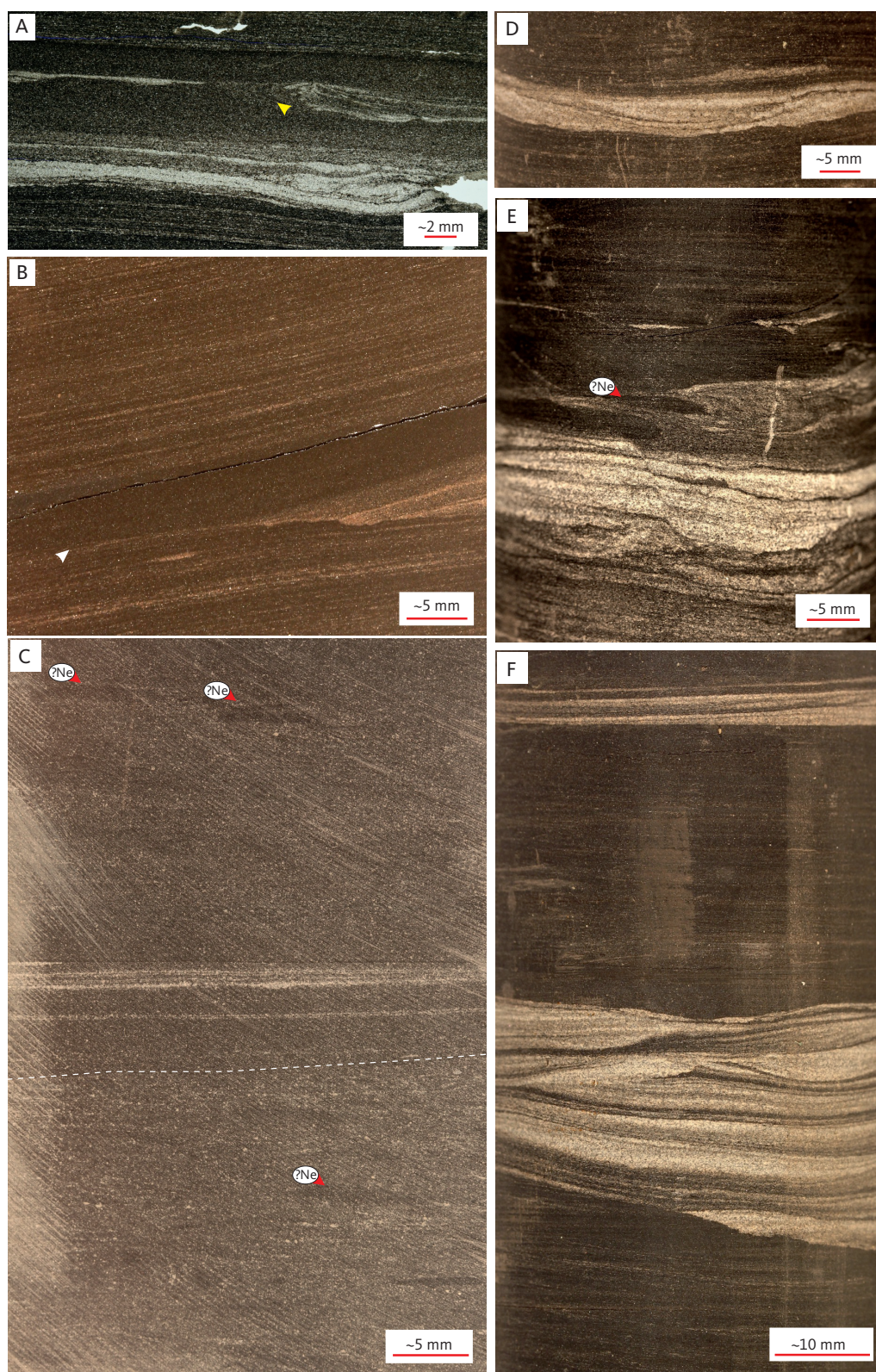


**Fig. 7** Facies F2B and F3. **A:** Normally graded sand-mud laminae sets with structureless mud laminae. Yellow arrow points to syn-sedimentary deformation including small-scale slump folding. Rødryggen-1, 233.69 m. **B:** A sand-filled scour (F3) grading laterally into mud-on-mud contact. The scour is interbedded with laminated silt and clay of F2B. Brorson Halvø-1, 135 m. **C:** Mud-rich heteroliths (F2B), interbedded bioturbated intervals. **White-dashed line** marks the base of a structureless mud lamina. **?Ne:** possible *Nereites*. Brorson Halvø-1, 185.5 m. **D:** Ripple cross-lamination showing laminae offshoots typical for wave ripples (F3). Brorson Halvø-1, 147 m. **E:** Cross-lamination with bioturbated top (F3). Brorson Halvø-1, 185 m. **F:** A scour-and-fill structure with ripple cross-laminated top (F3). The structure is interpreted as a storm wave-modified gravity deposit. Brorson Halvø-1, 183.5 m.



Two different types of erosionally based, normally graded lamina sets and beds are present. Type (1) comprises a few millimetre-thick siltstone–claystone couplets that show locally a tripartite microstructure: a basal micro-scoured contact below a millimetre-scale coarse siltstone or very fine-grained sandstone lamina (unit A; Fig. 6C, D). This basal lamina shows lateral thickness variability, pinch-outs and may contain inclined sub-millimetre thick mud drapes. The basal unit A is abruptly overlain by millimetre-thick parallel-laminated claystone and siltstone (unit B in Fig. 6D), which further grades into a structureless clayey mud-drape (unit C in Fig. 6D) that may contain pyrite. Type (2) comprises tabular, sharp-based siltstone–claystone laminae/beds. These beds are clay-dominated and appear to be composed of two components: a basal, c. 0.5–2 mm thick lenticular silt layer, which may contain inclined mud drapes and grades upwards into a structureless millimetre- to centimetre-scale clay bed. The basal contact in the Type 2 beds lacks evidence of prominent erosion.

In addition to the upward-fining lamina couplets and triplets, F2B shows subtle changes locally in lamina angle, lamina truncations and on-lapping or top-lapping lamina contacts, particularly where the facies is interbedded with cross-laminated sandstone (F3; Fig. 6F–H). Locally, silt–clay laminae sets show subtle changes in lateral thickness (Fig. 6H). Soft-sediment deformation is also very common and occurs as millimetres- to centimetre-scale micro-slump units (contorted Z-shaped lamina). Sphaerulitic cracks are rarely observed.

The deposits commonly appear unbioturbated, though exhibiting locally a low-density or diversity trace fossil fabric similar to that of subfacies F2A (Fig. 6E). The differences include lowered and fluctuating bioturbation intensity (BI 0–3) and increasing burrow diameter of burrow mottling in F2B (from sub-millimetre- to millimetre-scale). Moreover, in a few cases, an assemblage comprising *Nereites*, *?Chondrites* and *Phycosiphon* was observed at the top or in between event laminae or beds, at the gradation to F3 (Fig. 7C).

**Interpretation:** The deposits are interpreted to be mainly related to various gravity-flow and wave-modified gravity-flow processes, but an influence from more sustained current systems is also possible. The heterolithic interlamination showing subtle changes in lamina angle, lamina truncations and down-lapping to top-lapping lamina contacts (Figs 6G, H) suggests the presence of compacted, low relief mud-floccule ripples (Macquaker & Bohacs 2007; Schieber *et al.* 2007; Schieber & Southard 2009). The silt–clay interlamination with laminae pinch-outs and lenticularity (Fig. 6H) is similar to that generated by Yawar & Schieber (2017) in a flume tank experiment. Their results showed that such clay–silt interlamination can

form under similar flow velocity as mud-floccule ripples, but with a lower sedimentation rate.

The Type 1 erosionally based graded lamina set with the locally visible tripartite microstructure (Figs 6C, D) is very similar to the wave-enhanced gravity-flow deposits described by Macquaker *et al.* (2010). They proposed a three-phase flow model to explain the formation of these structures. In phase 1, wave-induced turbulence and resuspension form an erosionally based sand or coarse silt lamina (unit A). In phase 2, the increasing sediment concentration in the wave boundary layer damps turbulence, a pressure gradient develops and gravity flow begins. Shear mixing at the base of the laminar flow and mixing with sediment already in suspension results in the deposition of interlaminated silt and clay (unit B). In phase 3, the flow energy wanes, and the lutocline collapses (i.e. the suspended mud cloud), flow stops and the deposits grade into a clay-rich layer (unit C). Alternatively, such a structure could be deposited from a muddy gravity-flow current below wave base, which would also lead to turbulence damping as the flow decelerates and mud concentration increases (cf. Baas *et al.* 2011). The wave-enhanced gravity-flow interpretation is supported here by the fact that the deposits either grade into or are interbedded with, wave-rippled sandstone (F3) and gutter casts (see Section 4.1.3).

The Type 2 normally graded, tabular siltstone–claystone beds that lack prominent erosional scour at the base are interpreted as muddy gravity-flow deposits related to an increasing sea-floor gradient during episodes of block rotation. This interpretation is supported by the presence of intercalated slump deposits (F7). However, given the close association with deposits showing wave-influenced sedimentary structures, it is also possible that wave energy had a role in the formation of these deposits, and that the lack of unit B in these beds could be due to the dominance of clay, rapid flow deceleration or both.

The locally occurring *Nereites*-bearing ichnofabric and increasing burrow diameter suggest that oxygen levels increased at times during the deposition of F2B to F3. Fluctuating bioturbation intensity and soft-sediment deformation are also compatible with elevated depositional rates and common small-scale event deposition. The abundant coaly material and plant debris point to distal fluvial influence. This is corroborated by Hydrogen Index and C30 desmethyl sterane trends, which reveal an elevated input of terrigenous organic matter (Bojesen-Koefoed *et al.* 2023, this volume).

Additionally, considering the sedimentological and ichnological characteristics as well as the stratigraphic position of the facies above dysoxic offshore sediments (F2A), F2B is interpreted to reflect deposition in a wave-influenced and fluvially sourced and tectonically

active proximal offshore environment with a variable sea-floor gradient.

#### 4.1.3 Facies F3: cross-laminated sandstone

*Description:* F3 is a subordinate, but recurring facies type in both cores. It forms a few millimetres to a centimetre thick and is commonly interbedded with F2. It is typically present in the upper part of coarsening-upward successions (See 5. Discussion). F3 consists of ripple cross-stratified siltstone and very fine-grained sandstone. The ripples are characterised by asymmetrical to symmetrical profiles, irregular lower-bounding surfaces and common foreset offshoots that persist across the trough between ripples and peak again on the next ripple (Fig. 7D). Locally, the cross-laminated facies show a laterally variable erosional lower boundary forming scour-and-fill structures that are a few centimetres thick (Figs 7B, F). The basal contact may be overlain by parallel-laminated, cross-stratified siltstone or very fine-grained sandstone onlapping the laterally limited basal scour. At the top, the siltstone–sandstone unit may be overlain by clay-rich mud drapes up to 1 cm thick (Figs 7B, F). On the GR log, F3 is not always clearly expressed (due to the thin layers) but shows variable values of c. 80–120 API. F3 is commonly unbioturbated. In a single example, probable *Nereites* intensively burrow the overlying mud drape (BI 0–5).

*Interpretation:* Irregular lower bounding surfaces, bundling of laminae, foreset offshoots and locally occurring symmetrical ripple profiles suggest wave influence in the formation of the ripples (e.g. Reineck & Singh 1986). The laterally limited, relatively deep scour-and-fill structures showing onlapping lamina contacts over the basal erosional surface are interpreted to be storm-generated gutter casts (Myrow *et al.* 2002).

#### 4.1.4 Facies F7: slumps

*Description:* In the Brorson Halvø-1 core section, F7 is a common facies type in the lower Volgian of the Bernebjerg Formation and a dominant facies in the middle Volgian Lindemans Bugt Formation. It forms decimetre-to metre-scaled intervals and consists of slumped mudstone (F1) or heterolithic sediments (F2; Fig. 5C).

*Interpretation:* F7 is interpreted to record downslope mass wastage due to episodes of increased sea-floor gradients under block rotation.

### 4.2 Palnatokes Bjerg Formation

The Palnatokes Bjerg Formation in the two cored boreholes consists of two facies: F4 of the Albrechts Bugt Member and F5 of the Rødryggen Member. The latter only occurs in the Brorson Halvø-1 borehole and is subdivided into two subfacies.

#### 4.2.1 Facies F4: bioturbated calcareous mudstone

*Description:* F4 is a broad facies type, which forms the Albrechts Bugt Member interval. It is dominated by bioturbated fossiliferous mudstone, which has a variable amount of sand and calcite cement in the matrix. Locally, the deposits consist of variably bioturbated interlaminated grey mudstone and light grey calcareous mudstone. Near the top of the Albrechts Bugt Member, the facies appears structureless and contains shell fragments. F4 is generally characterised by a high fossil content. *Buchia* bivalves are especially common. Lithological accessories include abundant pyrite.

F4 is typically intensively bioturbated (BI 3–6) with a relatively low-diversity trace fossil assemblage dominated by *Zoophycos* and *Chondrites* of various sizes or cryptobioturbation (Fig. 8A, B). *Chondrites* cross-cut or reburrow other trace fossils. Secondary trace fossils include palimpsest grazing structures as well as rare *Siphonichnus* and *Thalassinoides* (Figs 8B, C).

*Interpretation:* The ubiquitous biogenic reworking in this facies precludes detailed process interpretation. However, given the depositional setting, grain size and the nature of the underlying succession, it is likely that hemipelagic settling and dilute gravity-flow processes were prevalent. The change from the unburrowed black mudstones of the Lindemans Bugt Formation to the fully bioturbated calcareous mudstones of the Albrechts Bugt Member points to an environmental shift from an anoxic basin to an oxic basin with limited input of clastic sediment. The very low clastic sediment input is interpreted to be due to the late syn-rift paleogeographic configuration (compartmentalised basin) and eustatic sea-level rise (Surlyk 1978). In summary, F4 is interpreted to represent sediment-starved deposits in a transgressed tilted fault-block setting.

#### 4.2.2 Facies F5: red calcareous mudstone

*Description:* F5 forms the Rødryggen Member interval in the Brorson Halvø-1 borehole. It consists of bioturbated red mudstone (Fig. 8D–G), which has a variable carbonate content in the matrix; earlier works have shown that the red colour is due to haematite (Alsen 2006). F5 is typically fully bioturbated (BI 6) exhibiting *Zoophycos*, *Chondrites*, *Siphonichnus*, ?*Nereites* and burrow mottling.

Facies F5 is divided into 2 subfacies. The first, F5A, consists of intensively bioturbated (burrow mottled), structureless red mudstone (Fig. 8F). Sand content is variable. The second subfacies, F5B, comprises bioclast-rich red mudstone and is characterised by a lower and fluctuating bioturbation intensity (BI 0–6). It contains sharp-based, shell hash beds that are a few centimetre thick (Fig. 8D). In addition, dispersed *Inoceramus*

fragments with borings (Fig. 8G) and millimetre-scale rounded mud-clasts are very common locally.

**Interpretation:** The strongly composite biogenic fabric and the trace fossil assemblage point to a condensed, relatively deep, marine environment. The sharp-based shell-hash beds and locally incomplete bioturbation intensity in F5B are indicative of event deposition, probably due to gravity-flow events on a slope. Earlier field-work has demonstrated that the Rødryggen Member is restricted to fault-block crests (Surlyk 1978). Given the sedimentological and ichnological evidence discussed here, F5 is interpreted to record sedimentation on an oxygenated submarine high in a deep marine setting (See 5. Discussion).

### 4.3 Stratumbjerg Formation

In the two borehole sections presented here, the Stratumbjerg Formation is represented only in the uppermost levels of the Brorson Halvø-1 core.

#### 4.3.1 Facies F6: bioturbated mudstone

**Description:** The interval referred to F6 in the Brorson Halvø-1 core is poorly preserved, consisting mainly of rubble. It comprises fully bioturbated (BI 6) light grey to greenish mudstone (Fig. 8G). The deposits contain *Chondrites* of different sizes, diminutive *Zoophycos*, palimpsest grazing structures (*Helminthopsis* and ?*Nereites*) and rare *Thalassinoides*. *Chondrites* commonly re-burrow other trace fossils. *Inoceramus* fragments and pyrite are common. The mudstone has a variable carbonate content, and concretionary beds are present locally.

**Interpretation:** The fine-grained lithology, the fully bioturbated fabric, the present ichnogenes and the lack of other forms suggest sub-storm wave-base basinal environment. The trace fossil content is not essentially different from that of the underlying Palnatokes Bjerg Formation. In outcrop, the Stratumbjerg Formation is characterised by a regionally extensive grey mudstone succession with occasional thin sandy turbidites (Bjergager *et al.* 2020). Thus, the F6 mudstone facies in the uppermost Brorson Halvø-1 core probably represents a transitional variant recording the initial change towards renewed clastic sediment deposition in the area.

## 5. Discussion

The two drill cores provide an insight into mud accumulation in a distal fault block through almost a full rift cycle. Whereas most of the previous research in the area has concentrated on characterisation of the coarse-grained gravity-flow systems in the coast-attached proximal fault block (e.g. Surlyk 1978; Henstra *et al.* 2016), the coeval sediments in distal areas have remained poorly

documented. Notably, distal sediments corresponding to the rift-climax phase were practically unknown prior to this drilling program.

The facies recorded in the cores are diverse, reflecting sedimentation in the following settings: (1) storm-affected, oxygen-depleted deltaic shelf (Bernbjerg Formation; Fig. 9A); (2) basin floor and slope in a dysoxic-anoxic half-graben (Lindemans Bugt Formation; Fig. 9B) and (3) sediment-starved deep half-graben under oxic conditions (Palnatokes Bjerg Formation). Finally, the top Brorson Halvø-1 core extends into the Barremian, which records the gradation to (4) regionally continuous basinal mud accumulation under waning rifting (Stratumbjerg Formation).

Recently, Hovikoski *et al.* (2023) summarised the depositional and tectonostratigraphic evolution of the black mudstone succession and broad-scale changes in bottom oxygenation during the rifting. Here, we revisit the depositional evolution and further discuss the main facies.

### 5.1 Bernbjerg Formation (Kimmeridgian – lower Volgian)

The sedimentary facies indicate that the Bernbjerg Formation represents an essentially aggradational muddy shelf succession that was fed by fine-grained fluvial systems (Fig. 9A; see also Surlyk & Clemmensen 1983). In addition to macroscopic observations of common coalified wood fragments and plant debris, the prodeltaic nature is well-documented by organic geochemistry data, which indicate a prominent input of terrigenous organic matter (Bojesen-Koefoed *et al.* 2023, this volume; Hovikoski *et al.* 2023). The seaway was influenced by south-orientated axial currents (Hovikoski *et al.* 2023), which allowed along-coast dispersal of the river-supplied sediments. The Upper Cretaceous Dunvegan Formation of Canada represents an analogous scenario (Plint 2014). Water depth ranged from a sub-storm wave-base offshore setting (F1; mainly laminated mudstone) to proximal offshore (F2B, F3; cross-laminated heteroliths and sandstone) and incipient slope environments (F7; slumps) below and above storm wave-base. The slope environment started to evolve, especially during the early Volgian when rifting accelerated. Elemental redox data and the distribution of bioturbation indicate fluctuating redox conditions in a generally hypoxic setting (see Hovikoski *et al.* 2023).

Facies alternations occur on several scales ranging from millimetre- to centimetre-scale facies alternations to depositional or tectonic cycles up to several tens of metres thick. The formation consists of several subtle, irregular transgressive-regressive and regressive cycles c. 10–30 m thick that individually comprise apparently chaotic facies alternations and rare, poorly developed higher-frequency depositional successions some metres



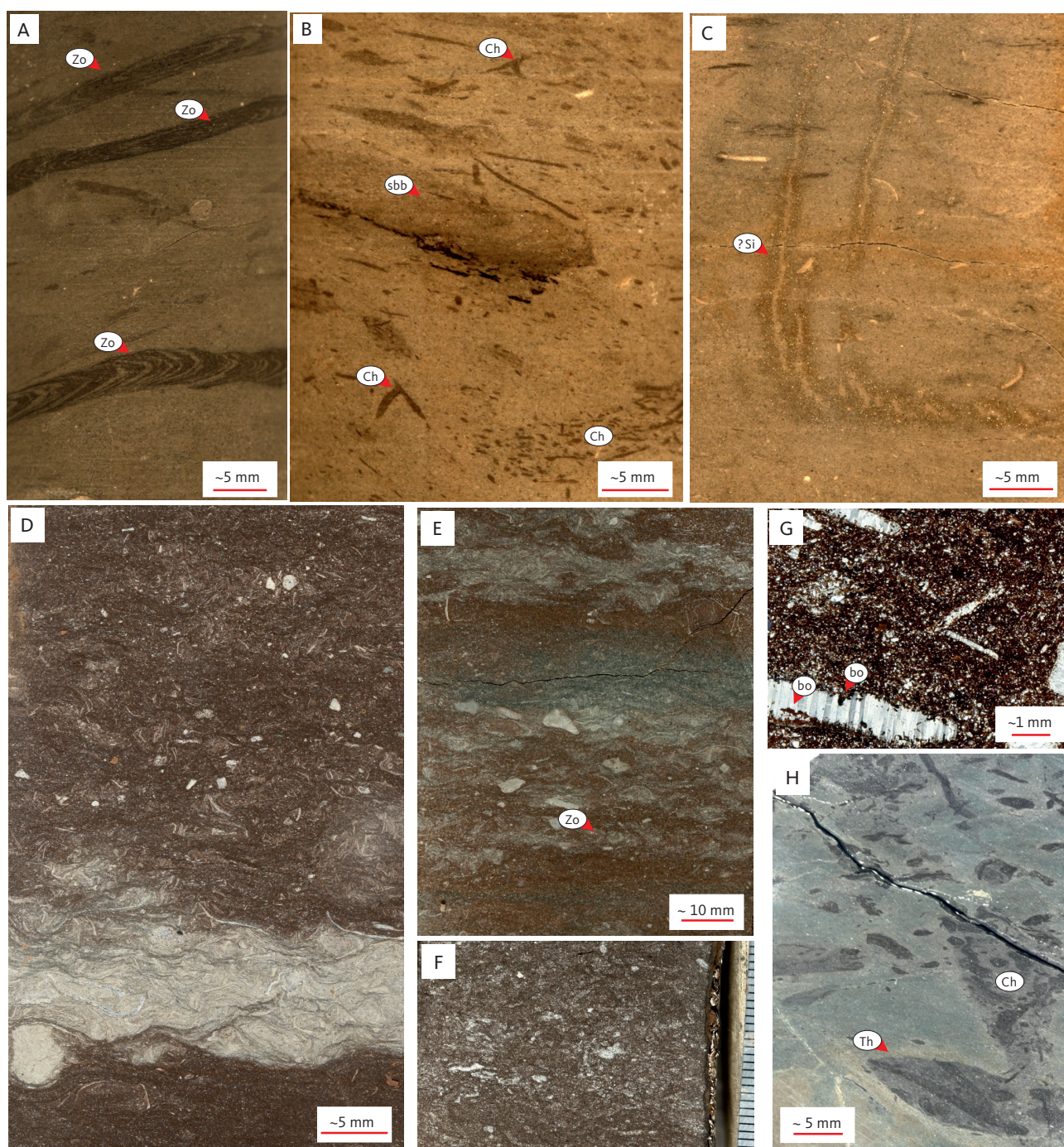


**Fig. 8** **A–C:** Examples of bioturbated marl (F4) characteristic of the Albrechts Bugt Member. Panel A is dominated by *Zoophycos* (**Zo**), whereas B illustrates common *Chondrites* (**Ch**) that cross-cut and re-burrow palimpsest traces. **sbb**: – spreite-bearing burrow potentially representing *Rhizocorallium*. C shows potential pyritised *Siphonichnus* (**?Si**). A and B from Rødryggen-1, interval around 20.5 m; C from Rødryggen-1, 10.5 m. **D–G:** Facies examples of red bioclast-rich mudstones of the Rødryggen Member (F5). Panels D and E show occasional shell beds and scattered shell fragments in variably burrow-mottled fabric (F5B). Visible traces include *Zoophycos*. F illustrates intensively bioturbated structureless red mudstone (F5A). Panels D, E and F from Brorson Halvø-1, 20 m, 22 m and 28 m, respectively. Panel G is a thin section micrograph illustrating bored (**bo**) inoceramid fragments in sandy mudstone. Brorson Halvø-1, 9.7 m. **H:** Bioturbated grey mudstone (F6) from the basal part of the Stratumbjerg Formation. Two size classes of *Chondrites* reburrowing *Thalassinoides* (**Th**). Brorson Halvø-1, 6.5 m.

thick. An ideal, major upward-coarsening succession consists of F1, F2A, F2B and F3, reflecting progradation from dominantly low-energy dysoxic offshore conditions to proximal offshore with a higher frequency of depositional events. This ideal coarsening-upward trend is complicated by syntectonic influence, which affected

depositional rate, bottom gradient, water depth and sediment source areas. Particularly from the lower Volgian and on, contrasting depositional rates are recorded by the two cores: The *P. elegans* – *P. wheatleyensis* ammonite chronozone interval is c. 30 m thick in the Rødryggen-1 core, whereas the corresponding interval in the



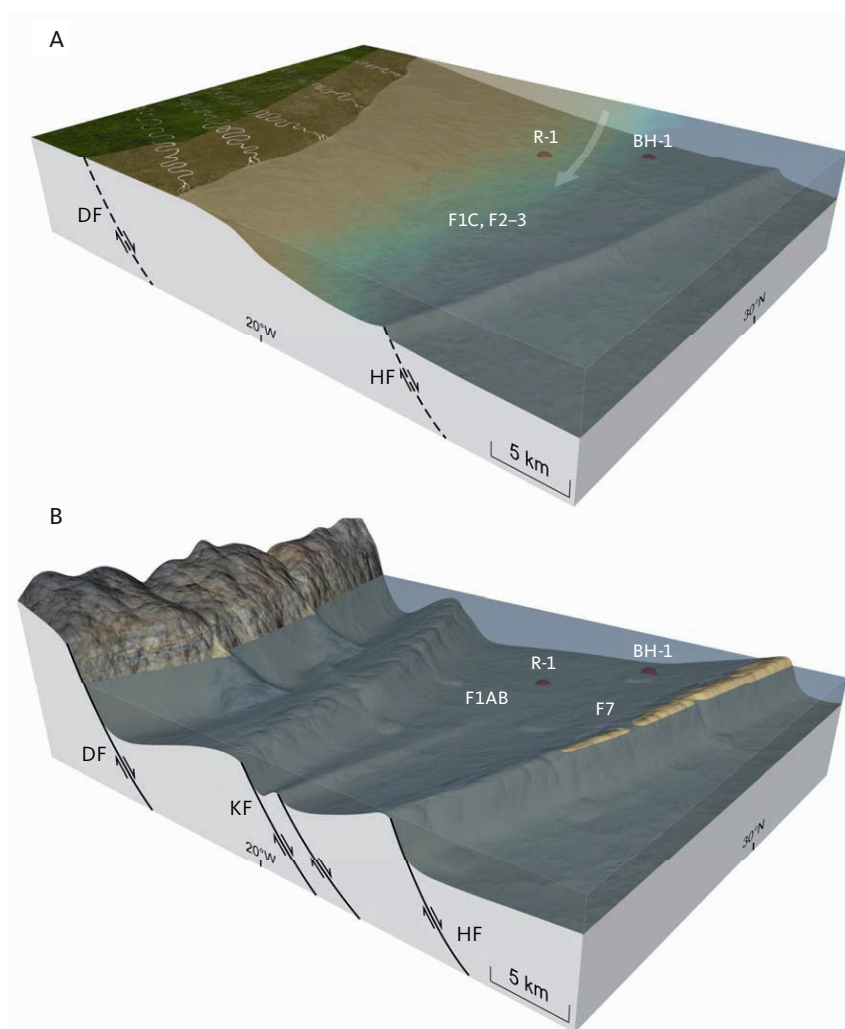


**Fig. 9** Tectonostratigraphic–depositional scenarios of the Wollaston Forland area during the Late Jurassic – Early Cretaceous (modified from Hovikoski *et al.* in 2023). **A:** Kimmeridgian fluvially-sourced shelf influenced by along-coast sediment dispersal. The arrow indicates the main sediment transport direction, and red dots indicate borehole positions. **DF:** Dombjerg fault. **HF:** Hühnerbjerg fault. **B:** Middle Volgian – Ryazanian half-graben. The model shows major uplift along the Dombjerg fault and the development of the coarse-grained fan deltas of the Rigi Member (Lindemans Bugt Formation) in the coastal fault block (Surlyk 1978, 2003). The fan delta-related gravity flows were blocked by the uplifted Kuppel fault (**KF**) crest, which defined the western margin of the Permpas/Hühnerbjerg block(s). The hiatuses present in the Brorson Halvø-1 core indicate coeval uplift pulses along the Hühnerbjerg block crest. **R-1:** Rødryggen-1 borehole. **BH-1:** Brorson Halvø-1 borehole. Subfacies **F1C** and **F1AB** along with facies **F2-3** and **F7** are shown.

Brorson Halvø-1 core is >100 m thick (Alsen *et al.* 2023, this volume). Due to these factors, as well as increasing clay laminae thickness in higher energy facies (F3), the coarsening-upward successions are commonly poorly expressed on the GR log.

Fining-upward successions related to transgressive phases are best developed in the lower part of the Bernbjerg Formation (Kimmeridgian). These successions characteristically contain F1C beds, interbedded with F1B or F2. On the GR log, the successions are only weakly developed but are identifiable as serrated, generally increasing GR trends, punctuated by recurrent beds with low GR values (e.g. Brorson Halvø-1, 202–195 m). The stacking patterns of the major cycles suggest a maximum flooding zone in the upper part of the Kimmeridgian, around 178 m in the Brorson Halvø-1 core. This is followed by an overall progradational trend, the zone

of maximum regression being situated at around 100 m, in the lower Volgian *P. elegans* zone.

#### 5.1.1 Sedimentary event beds and laminae

Although the lithology of the Bernbjerg Formation is generally fine-grained, indications of erosion, laminae-scale event deposition and traction currents are widespread. Event deposition is recorded as wave ripples, scour-and-fill structures (gutter casts), convergent lamination pointing towards putative mud floccule ripples (Schieber *et al.* 2007) and associated silt-clay interlamination with pinch-outs and lenticular laminae (Figs 6, 7; Yawar & Schieber 2017). Furthermore, normally graded siltstone–claystone beds, interpreted as muddy gravity flows, and probable wave-enhanced gravity-flow deposits occur frequently (Macquaker *et al.* 2010; Plint 2014). Although similar structures may result from pure gravity-flow processes



below wave-base, their close association with gutter casts and wave ripples points to the involvement of storm-wave processes. Such structures are also missing from the Lindemans Bugt Formation, which is interpreted to represent a sub-storm wave-base basinal and slope environment (see Section 5.2).

Clay-rich mud layers can be up to 1 cm thick at the top of normally graded event beds. Their structureless and seemingly ungraded nature coupled with common soft sedimentary deformation features (loading, slump-folding) suggest high water content and probably a fluid mud component in sedimentation.

Many sand-bearing event beds such as gutter casts pinch-out rapidly and are laterally equivalent to mud-on-mud contacts. The mud-rich ripples range from well-defined cross-lamination with sand interlaminae (Fig. 6H) to subtle silt-clay laminae sets showing lateral thickness variations and convergent laminae (Fig. 6F, G). Such occurrences are commonly observed adjacent to small, laminae-confined slump intervals, which may suggest that an increased slope gradient enhanced the mud-ripple development.

Overall, the observed facies are similar to those reported from other storm-affected Mesozoic mudstone successions, including the Cretaceous Dunvegan Formation (Plint 2014) and the Mowry shale (Macquaker *et al.* 2010; Lazar *et al.* 2022) from the Western Interior Seaway. Other examples include the Jurassic Cleveland Ironstone Formation, the Whitby Mudstone Formation (Ghadeer & Macquaker 2011) and some intervals of the Kimmeridge Clay Formation, UK (e.g. Wignall 1989; Macquaker & Gawthorpe 1993).

## 5.2 Lindemans Bugt Formation (middle Volgian – late Ryazanian)

In the Brorson Halvø core, the base of the Lindemans Bugt Formation is marked by a major hiatus or stratigraphic condensation as indicated by biostratigraphic data (Alsen *et al.* 2023, this volume). Similarly, the upper boundary of the formation is demarcated by a hiatus spanning from the middle Volgian to the late Ryazanian. These unconformities testify to further intensified tectonic activity in the Wollaston Forland area during the middle Volgian (Surlyk 1978, 2003). This rift climax resulted in tilted fault-block development and basin segmentation, lasting until the early late Ryazanian. The Brorson Halvø-1 borehole is situated near the elevated hanging-wall crest of the Permpas fault block about 30 km east of the main fault zone (the Dombjerg fault). During the middle Volgian, major conglomeratic fan deltas developed east of the Dombjerg fault (Surlyk 1978; Henstra *et al.* 2016). The eastern limit of the submarine fan delta deposits was controlled by the Kuppel Fault, which defined the western margin of

the Permpas block (Figs 1 and 9B). Due to basin segmentation and changes in sediment source areas, the Permpas block became isolated from the main focus of deltaic sedimentation and received progressively less terrestrial clastic sediment during rifting. This is directly reflected in the sedimentary facies exhibited by the Brorson Halvø-1 core, which suggest transformation into a non-deltaic, drowned oxygen-restricted slope (F7: slump) sub-storm wave-base slope (F1A, B: structureless to laminated mudstone) during the middle Volgian. The presence of the two major hiatuses resulted from reduced accommodation caused by uplift of the block crest.

## 5.3 Palnatokes Bjerg and Stratumbjerg Formations

The change from the Lindemans Bugt Formation to the Albrechts Bugt Member (Palnatokes Bjerg Formation) in the Rødryggen-1 core is gradational, occurring within 1 m of this boundary—a major hiatus in the Brorson Halvø-1 section. Above this boundary, the clastic sediment input decreased, and the environment became oxygenated as indicated by bioturbation and elemental redox proxies (Hovikoski *et al.* 2023). The change from black mudstone deposition to a ventilated basin with calcareous sedimentation is recognised supraregionally as an oceanographic change accompanied by the appearance of nannofossils with Tethyan influence (Pauly *et al.* 2013).

The interpretation of limited clastic input and low sedimentation rate is supported by the increased fossil content, increased bioturbation intensity, composite ichnofabrics (cross-cutting, re-burrowing) and the nature of the ichnofauna (*Zoophycos*- and *Chondrites*-dominated, low diversity ichnofabric). Moreover, the estimated bulk depositional rates are low (Hauterivian depositional rate c. 5.6 m/Myr; Hovikoski *et al.* 2023). In comparison to coeval outcrop data from the proximal fault block (Hovikoski *et al.* 2018), land-derived turbidites are absent, indicating continued detachment from coastal depositional systems in the studied fault block.

In the Brorson Halvø-1 section, the Albrechts Bugt Member grades into the Rødryggen Member at around 30 m depth, marked by a shift in the sedimentary facies to red bioclastic mudstones. Sedimentary facies suggest a more common gravity-flow component than in the Albrechts Bugt Member suggestive of an increasing slope gradient and a rift pulse or multiple rift pulses.

Piasecki *et al.* (2020) recently described coarse clastic sediments of the Falske Bugt Member (Palnatokes Bjerg Formation) near the Falkebjerg ridge, some kilometres east of the Brorson Halvø-1 drill site (Fig. 1), indicative of intensified rift activity in this region during the Valanginian–Barremian. Barremian syn-rift conglomerates are

not known from western fault systems (e.g. Dombjerg Fault), potentially suggesting that the rift climax persisted longer in the east. Unlike the deposits of the Falske Bugt Member, the coeval gravity flows of the Rødryggen Member comprise bioclasts and mud-clasts pointing to a limited or absent extraformational sediment source. This observation is compatible with localised footwall uplift and a compartmentalised basin.

The setting gradually returned to an oxygen-restricted, sub-storm wave-base, deep basinal environment during the late Hauterivian (basal Stratum Bjerg Formation, F6). The sediments record decreasing biogenic carbonate accumulation and the renewed increase in clastic sediment input. In outcrop, the basal boundary of the Stratum Bjerg is variably developed, being either conformable, as observed in the Brorson Halvø-1 core, or hiatal, eroding into the Bernbjerg Formation (Bjerager *et al.* 2020). In Wollaston Forland, this contact records waning rift activity, increased thermal subsidence and disappearance of rift-basin morphology.

## 6. Conclusions

The Rødryggen-1 and Brorson Halvø-1 drill cores offer an insight into marine mud accumulation in an evolving distal fault block. The full core recovery, almost pristine preservation of the facies, stratigraphic continuity and the well-established biostratigraphic framework make the cores one of the best stratigraphic-sedimentological data points of the Jurassic–Cretaceous boundary and Kimmeridge Clay equivalent in northern high latitude regions. In particular, the Kimmeridgian – lower Volgian hypoxic shelf setting allowed exceptional preservation of subtle sedimentary structures in very thinly bedded mudstones recording distinct depositional events and traction currents and contributing to a general understanding of the processes governing mud accumulation.

The cores document that black mudstone accumulation extended through the Kimmeridgian – early Ryazanian (late) early rift and rift climax phases (Bernbjerg and Lindemans Bugt Formations). The facies suggest that the early rift hypoxic prodeltaic shelf was characterised by suspension settling, starved wave ripples, scour-and-fill structures, putative mud floccule ripples and mud-dominated gravity-flow deposits. During the rift climax phase, the depositional environment evolved into a narrow half-graben characterised by bioclastic and pyrite-rich black mudstones. These deposits document hemipelagic suspension settling and gravity-flow or mass-wasting deposition in sub-storm wave-base, dysoxic, anoxic to euxinic slope and basin-floor environments.

The Ryazanian–Valanginian late syn-rift setting experienced a supra-regional oceanographic change and improved ventilation, which is reflected in the deposition

of deep marine marls (Albrechts Bugt Member, Palnatokes Bjerg Formation). Condensed, red bioclastic mudstones with a common gravity-flow component characterised the Hauterivian, which probably recorded an eastward shift in fault activity and final blanketing of the submerged fault-block crest (Rødryggen Member, Palnatokes Bjerg Formation). The top of the cored succession is marked by the appearance of dark grey bioturbated mudstones of Barremian age, recording the onset of regionally continuous deep marine clastic mud accumulation in thermally subsiding basins.

Thus, although superficially monotonous, detailed facies analysis of the mudstone-dominated succession exhibited by the Rødryggen-1 and Brorson Halvø-1 boreholes reveals a highly dynamic depositional system that reflects shifting marine processes under varied hydrodynamic conditions, at different water depths and varied levels of bottom oxygenation during almost a full rift cycle.

## Acknowledgements

Jette Halskov, Stefan Solberg and Jacob L. Bendtsen are thanked for professional graphic support. Guy Plint and Paul Smith are thanked for constructive and insightful reviews.

## Additional information

### Funding statement

Funding for drilling of the Rødryggen-1 and Brorson Halvø-1 boreholes and studies of the cores was provided by a consortium of oil companies and the Geological Survey of Denmark and Greenland (GEUS).

### Author contributions

JH: wrote the paper in co-operation with other authors. JH and JL: sedimentology. MO: Mineralogy and diagenesis. JBK: organic geochemistry. SP and PA: biostratigraphy.

### Competing interests

The authors declare no competing interests.

### Additional files

None provided.

## References

- Alsen, P. 2006: The Early Cretaceous (Late Ryazanian – Early Hauterivian) ammonite fauna of North-East Greenland: Taxonomy, biostratigraphy, and biogeography. *Fossils & Strata* **53**, 229 pp. <https://doi.org/10.18261/9781405180146-2006-01>
- Alsen, P., Piasecki, S., Nøhr-Hansen, H., Pauly, S., Sheldon, E. & Hovikoski, J. 2023: Stratigraphy of the Upper Jurassic to lowermost Cretaceous in the Rødryggen-1 and Brorson Halvø-1 boreholes, Wollaston Forland, North-East Greenland. *GEUS Bulletin* **55**, 8342 (this volume). <https://doi.org/10.34194/geusb.v55.8342>
- Baas, J.H., Best, J.L. & Peakall, J. 2011: Depositional processes, bedform development and hybrid bed formation in rapidly decelerated cohesive (mud-sand) sediment flows. *Sedimentology* **58**, 1953–1987. <https://doi.org/10.1111/j.1365-3091.2011.01247.x>
- Bentley, S.J. & Nittrouer, C.A. 2003: Emplacement, modification, and preservation of event strata on a flood-dominated continental shelf:



- Eel Shelf, northern California: Continental Shelf Research **23**(19), 1465–1493. <https://doi.org/10.1016/j.csr.2003.08.005>
- Bjerager, M. *et al.* 2020: Cretaceous lithostratigraphy of North-East Greenland. *Bulletin of the Geological Society of Denmark* **68**, 37–93. <https://doi.org/10.37570/bgsd-2020-68-04>
- Bojesen-Koefoed, J.A., Alsen, P., Bjerager, M., Hovikoski, J., Ineson, J.R., Johannessen, P., Olivarius, M., Piasecki, S. & Vosgerau, H. 2023a: The Rødryggen-1 and Brorson Halvø-1 fully cored boreholes (Upper Jurassic – Lower Cretaceous), Wollaston Forland, North-East Greenland – an introduction. *GEUS Bulletin* **55**, 8350 (this volume). <https://doi.org/10.34194/geusb.v55.8350>
- Bojesen-Koefoed, J.A., Alsen, P., Bjerager, M., Hovikoski, J., Johannessen, P., Nøhr-Hansen, H., Petersen, H.I., Piasecki, S. & Vosgerau, H. 2023b: Organic geochemistry of an Upper Jurassic – Lower Cretaceous mudstone succession in a narrow graben setting, Wollaston Forland Basin, North-East Greenland. *GEUS Bulletin* **55**, 8320 (this volume). <https://doi.org/10.34194/geusb.v55.8320>
- Boyer, D. & Droser, M. 2011: A combined trace- and body-fossil approach reveals high-resolution record of oxygen fluctuations in Devonian seas. *Palaios* **26**, 500–508. <https://doi.org/10.2110/palo.2010.p10-073r>
- Ghadeer, S. & Macquaker, J. 2011: Sediment transport processes in an ancient mud-dominated succession: A comparison of processes operating in marine offshore settings and anoxic basinal environments. *Journal of the Geological Society (London)* **168**, 1121–1132. <https://doi.org/10.1144/0016-76492010-016>
- Henstra, G.A. *et al.* 2016: Depositional processes and stratigraphic architecture within a coarse-grained rift margin turbidite system: The Wollaston Forland Group, East Greenland. *Marine and Petroleum Geology* **76**, 187–209. <https://doi.org/10.1016/j.marpetgeo.2016.05.018>
- Hovikoski, J., Uchman, A., Alsen, P. & Ineson, J. 2018: Ichnological and sedimentological characteristics of submarine fan deposits in a half-graben, Lower Cretaceous Palnatokes Bjerg Formation, NE Greenland. *Ichnos* **26**(1), 28–57. <https://doi.org/10.1080/10420940.2017.1396981>
- Hovikoski, J. *et al.* 2023: Late Jurassic–Early Cretaceous marine deoxygenation in NE Greenland. *Journal of the Geological Society* **180**(3), jgs2022-058. <https://doi.org/10.1144/jgs2022-058>
- Ichaso, A.A. & Dalrymple, R.W. 2009: Tide- and wave-generated fluid mud deposits in the Tilje Formation (Jurassic), offshore Norway. *Geology* **37**, 539–542. <https://doi.org/10.1130/g25481a.1>
- Kineke, G.C., Sternberg, R.W., Trowbridge, J.H. & Geyer, W.R. 1996: Fluid mud processes on the Amazon continental shelf. *Continental Shelf Research* **16**, 667–696.
- Lazar, O.R., Bohacs, K.M., Schieber, J., Macquaker, J.H.S. & Demko, T.M. 2022: Laminae, laminasets, beds, and bedsets. In: Bohacs, K.M. & Lazar, O.R. (eds): *Sequence stratigraphy: Applications to fine-grained rocks*. AAPG Memoir **126**, 89–106.
- Macquaker, J. & Bohacs, K. 2007: On the accumulation of mud. *Science* **318**, 1734–1735. <https://doi.org/10.1126/science.1151980>
- Macquaker, J., Bentley, S. & Bohacs, K. 2010: Wave-enhanced sediment-gravity flows and mud dispersal across continental shelves: Reappraising sediment transport processes operating in ancient mudstone successions. *Geology* **38**, 947–950. <https://doi.org/10.1130/g31093.1>
- MacQuaker, J.H.S. & Gawthorpe, R.L. 1993: Mudstone lithofacies in the Kimmeridge Clay Formation, Wessex Basin, southern England; implications for the origin and controls of the distribution of mudstones. *Journal of Sedimentary Research* **63**(6), 1129–1143. <https://doi.org/10.1306/D4267CC1-2B26-11D7-8648000102C1865D>
- Martin, K.D. 2004: A re-evaluation of the relationship between trace fossils and dysoxia. In: McIlroy, D. (ed.): *The Application of Ichnology to Palaeoenvironmental and Stratigraphic Analysis*. Geological Society (London), Special Publications **228**, 141–156. <https://doi.org/10.1144/gsl.sp.2004.228.01.08>
- Myrow, P., Fischer, W. & Goodge, J. 2002: Wave-modified turbidites: Combined-flow shoreline and shelf deposits, Cambrian, Antarctica. *Journal of Sedimentary Research* **72**, 641–656. <https://doi.org/10.1306/022102720641>
- Nøhr-Hansen, H. 1993: Dinoflagellate cyst stratigraphy of the Barremian to Albian, Lower Cretaceous, North-East Greenland. *Grønlands Geologiske Undersøgelse Bulletin* **166**, 171 pp. <https://doi.org/10.34194/bullggu.v166.6722>
- Olivarius, M., Kazerouni, A.M., Weibel, R., Kokfelt, T.F. & Hovikoski, J. 2023: Mudstone diagenesis and sandstone provenance in an Upper Jurassic – Lower Cretaceous evolving half-graben system, Wollaston Forland, North-East Greenland. *GEUS Bulletin* **55**, 8309 (this volume). <https://doi.org/10.34194/geusb.v55.8309>
- Pauly, S., Mutterlose, J. & Alsen, P. 2013: Depositional environments of Lower Cretaceous (Ryazanian–Barremian) sediments from Wollaston Forland and Kuhn Ø, North-East Greenland. *Bulletin of the Geological Society of Denmark* **61**, 19–36. <https://doi.org/10.37570/bgsd-2013-61-02>
- Piasecki, S., Bojesen-Koefoed, J.A. & Alsen, P. 2020: Geology of the Lower Cretaceous in the Falkebjerg area, Wollaston Forland, northern East Greenland. *Bulletin of the Geological Society of Denmark* **68**, 155–169. <https://doi.org/10.37570/bgsd-2020-68-07>
- Plint, A.G., Macquaker, J.H.S. & Varban, B.L. 2012: Shallow-water, storm-influenced sedimentation on a distal, muddy ramp: Upper Cretaceous Kaskapau Formation, Western Canada foreland basin. *Journal of Sedimentary Research* **82**, 801–822.
- Plint, G. 2014: Mud dispersal across a Cretaceous prodelta: storm-generated, wave-enhanced sediment gravity flows inferred from mudstone microtexture and microfacies. *Sedimentology* **61**, 609–647. <https://doi.org/10.1111/sed.12068>
- Potter, P.E., Maynard, J.B. & Depetris, P.J. 2005: *Mud and Mudstones: Introduction and Overview*. 297 pp. Berlin: Springer-Verlag. <https://doi.org/10.2113/gsecongeo.100.7.1469>
- Potter, P.E., Maynard, J.B. & Pryor, W.A. 1980: *Sedimentology of Shale – Study Guide and Reference Source*. 306 pp. New York: Springer. <https://doi.org/10.1007/978-1-4612-9981-3>
- Reineck, H. & Singh, I. 1986: *Sedimentary Depositional Environments*. 683 pp. Berlin: Springer-Verlag. [https://doi.org/10.1016/0033-5894\(81\)90023-5](https://doi.org/10.1016/0033-5894(81)90023-5)
- Schieber, J. & Southard, J.B. 2009: Bedload transport of mud by floccule ripples – Direct observation of ripple migration processes and their implications. *Geology* **37**, 483–486. <https://doi.org/10.1130/g25319a.1>
- Schieber, J. & Wilson, R. 2021: Burrows without a trace – How meioturbation affects rock fabrics and leaves a record of meibenthos activity in shales and mudstones. *Paläontologische Zeitschrift* **95**, 767–791.
- Schieber, J. & Yawar, Z. 2009: A new twist on mud deposition – Mud ripples in experiment and rock record. *The Sedimentary Record* **7**, 4–8. <https://doi.org/10.2110/sedred.2009.2.4>
- Schieber, J., Southard, J. & Thaisen, K. 2007: Accretion of mudstone beds from migrating floccule ripples. *Science* **318**, 1760–1763. <https://doi.org/10.1126/science.1147001>
- Surlyk, F. 1978: Submarine fan sedimentation along fault scarps on tilted fault blocks (Jurassic–Cretaceous boundary, East Greenland). *Bulletin Grønlands Geologiske Undersøgelse* **128**, 108 pp. <https://doi.org/10.34194/bullggu.v128.6670>
- Surlyk, F. 1984: Fan-delta to submarine fan conglomerates of the Volgian–Valanginian Wollaston Forland Group, East Greenland. In: Koster, E.H. & Steel, R.J. (eds): *Sedimentology of gravel and conglomerates*. Canadian Society of Petroleum Geologists Memoir **10**, 359–382.
- Surlyk, F. 1990: A Jurassic sea-level curve for East Greenland. *Palaeogeography, Palaeoclimatology, Palaeoecology* **78**, 71–85. [https://doi.org/10.1016/0031-0182\(90\)90205-1](https://doi.org/10.1016/0031-0182(90)90205-1)
- Surlyk, F. 2003: The Jurassic of East Greenland: A sedimentary record of thermal subsidence, onset and culmination of rifting. In: Ineson, J.R. & Surlyk, F. (eds): *The Jurassic of Denmark and Greenland*. Geological Survey of Denmark and Greenland Bulletin **1**, 659–722. <https://doi.org/10.34194/geusb.v1.4674>
- Surlyk, F. & Clemmensen, L.B. 1975: A Valanginian turbidite sequence and its palaeogeographical setting (Kuhn Ø, East Greenland). *Bulletin of the Geological Society of Denmark* **24**, 61–73.
- Surlyk, F. & Clemmensen, L.B. 1983: Rift propagation and eustasy as controlling factors during Jurassic inshore and shelf sedimentation in northern East Greenland. *Sedimentary Geology* **34**, 119–143. [https://doi.org/10.1016/0037-0738\(83\)90083-0](https://doi.org/10.1016/0037-0738(83)90083-0)

- Surlyk, F. *et al.* 2021: Jurassic stratigraphy of East Greenland. *GEUS Bulletin* **46**, 6521. <https://doi.org/10.34194/geusb.v46.6521>
- Sykes, R.M. & Surlyk, F. 1976: A revised ammonite zonation of the Boreal Oxfordian and its application in northeast Greenland. *Lethaia* **9**, 421–436. <https://doi.org/10.1111/j.1502-3931.1976.tb00984.x>
- Taylor, A.M. & Goldring, R. 1993: Description and analysis of bioturbation and ichnofabric. *Journal of the Geological Survey (London)* **150**, 141–148. <https://doi.org/10.1144/gsjgs.150.1.0141>
- Vischer, A. 1943: Die Postdevonische Tektonik von Ostgrönland zwischen 74° und 75° n. *Br. Meddelelser om Grønland* **133**(1), 195 pp.
- Wignall, P.B. 1989: Sedimentary dynamics of the Kimmeridge Clay: Tempests and earthquakes. *Journal of the Geological Society* **146**(2), 273–284. <https://doi.org/10.1144/gsjgs.146.2.0273>
- Wright, L.D., Friedrichs, C.T., Kim, S.C. & Scully, M.E. 2001: Effects of ambient currents and waves on gravity-driven sediment transport on continental shelves. *Marine Geology* **175**, 25–45. [https://doi.org/10.1016/S0025-3227\(01\)00140-2](https://doi.org/10.1016/S0025-3227(01)00140-2)
- Yawar, Z. & Schieber, J. 2017: On the origin of silt laminae in laminated shales. *Sedimentary Geology* **360**, 22–34. <https://doi.org/10.1016/j.sedgeo.2017.09.001>